BIOCHEMISTRY
including biophysical chemistry & molecular biology

Article

pubs.acs.org/biochemistry

Structural Coupling between the Rho-Insert Domain of Cdc42 and the Geranylgeranyl Binding Site of RhoGDI

Adel Abramovitz, Menachem Gutman, and Esther Nachliel*

Laser Laboratory for Fast Reactions, Biochemistry and Molecular Biology department, Tel Aviv University, Tel Aviv, Israel 69978

Supporting Information

ABSTRACT: The small GTPase proteins are components of the intracellular signaling system, alternating between active (membrane-bound and GTP-loaded) and inactive (GDP-loaded and cytosolic) states. In the inactive state, the proteins are soluble in the cytoplasm. To compensate for the energetic penalty of extraction of the hydrophobic moiety from the membrane phase, the inactive state is stabilized via formation of a complex with the RhoGDI proteins that provide a hydrophobic pocket for the binding of the hydrophobic moieties. The signals delivered by the Rho subfamily involve a specific, short, highly exposed α-helix (Rho-insert), located close to the GDP binding site. Upon simulating the complex in solution, we observed that the Rho-insert domain of Cdc42 can assume two basic orientations. One is the canonical one, as detected in both crystals and NMR spectra of concentrated protein solutions. The second orientation appears only in the RhoGDI−Cdc42 complex where the GER moiety of Cdc42 is properly inserted into the specific binding site of RhoGDI. Any impairment of the GER−RhoGDI interactions, such as insertion of specific mutations in the hydrophobic binding site, abolished the coupling between the proteins and the Rho-insert domain, preserving its canonical orientation as in the crystalline structure. The noncanonical conformation of the Rho-insert domain is not a simulation artifact, as it appears in crystals of plant Rho proteins (ROP4, ROP5, and ROP7). In accord with the notion that the Rho-insert domain participates in downstream signaling, we propose that the deformation of the Rho-insert is part of the signal transmissions.

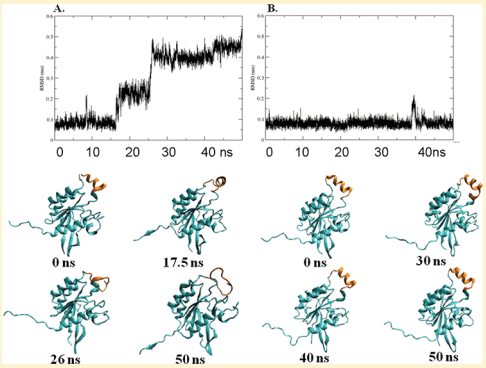

The Rho GTPases (guanine nucleotide binding proteins) serve as intracellular switching elements that regulate essential cellular processes such as cell migration, epithelial cell polarization, phagocytosis, and cell cycle progression.[1−4] The Rho family proteins are characterized by a hypervariable C-terminal tail that, frequently, is post-translationally modified by attachment of hydrophobic isoprenoid group (farnasyl or geranylgeranyl) moieties.[5,6] These moieties are instrumental in binding of the Rho protein to the membrane. The removal of Rho GTPase proteins from the cellular membrane and their stabilization in an inactive GDP-bound cytoplasmic state are achieved by the Rho guanine nucleotide dissociation inhibitor proteins (RhoGDIs). The crystallographic and nuclear magnetic resonance (NMR) structures of these proteins show a β-sandwich-like immunoglobulin motif of RhoGDI with a narrow hydrophobic cleft that binds the lipid moiety of the Rho proteins, thus compensating for the energetic penalty associated with its removal from the membrane.[7−12] In accord with the physiologic role of the Rho GTPases as signaling proteins, GDI binding is expected to affect the nature of the message delivered by the Rho protein to downstream effector proteins.[13−17] The structural deformation exhibited by the Rho protein, monitored by NMR spectroscopy,[18,19] revealed significant changes in the rigidity of the looser domains of the proteins (switch I, switch II, and the Rho-insert domain). Surprisingly, the variation in the flexibility of the Rho-insert was reported to be controlled by interactions at remote sites, suggesting that the protein in solution can exhibit an allosteric correlation between distant domains.[19] Accordingly, in this study, we investigated the structural changes that take place in the Rho protein, which are initiated by its interaction with GDI and are specific to the insertion of geranylgeranyl (GER) into the binding site of the GDI.

A unique structural element of all the members of the Rho subfamily (Rho, Rac, Cdc42, and others) is an α-helix of ∼13 residues located between β-strand 5 (β5) and helix 4 (α4) of Cdc42.[20,21] This helical section, also termed the Rho-insert region (RI), is not an integral part of the tight structure of the protein.[22−31] Removal of the RI region from the protein had an only minor effect on the stability of the protein, and the rate of GTP hydrolysis was hardly affected.[31] However, the Rho-insert was found to be crucial for the cellular functions of the protein.[26] The role of the Rho-insert in the activation of a downstream effector by the plant Rho protein (ROP) has been experimentally demonstrated,[32,33] confirming the suggestion that it serves as a binding interface for downstream effectors.[2,3,31,32,34,35] The assumption that the RI region is a recognition region for downstream effectors implies that structural fluctuations in this region may shift the Rho proteins

Received: August 4, 2011
Revised: December 25, 2011
Published: December 29, 2011

between the effective and noneffective states. In the absence of such a mechanism, the protein might be limited in its ability to alter its interaction with downstream proteins. Indeed, in a recent study looking at the nanosecond structural fluctuations of Rac1, significant changes in the order parameters of the Rho-insert domain were observed, demonstrating the feasibility of allosteric interactions between the effector protein binding site and the Rho-insert domain.[19]

The structure of the Rho proteins was determined by crystallization and NMR spectroscopy, and their structure concurs with a general configuration presented in Scheme 1. In this configuration, the Rho-insert domain appears at a given angle with respect to the main body of the protein. This orientation is common both for crystalline structures and for the solution structures determined by NMR. This configuration, the canonical one, is not affected by the crystallization conditions and common for an apoprotein or in the presence of GTP and GDP and in a concentrated solution of the protein.[37,38] However, the plant Rho proteins, ROP4, ROP5, and ROP7, were crystallized either in the canonical configuration or in another state, where the Rho-insert domain was rotated with respect to the main body of the protein.[27,39−42] Apparently, the Rho-insert may have more than one orientation, and considering the signaling function of this region, its alternation between the configurations may be physiologically significant. The transitions of the Rho-insert between these orientations are the subject of this study.

Scheme 1. Canonical Conformation of the Rho-Insert Helix in Cdc42[a]

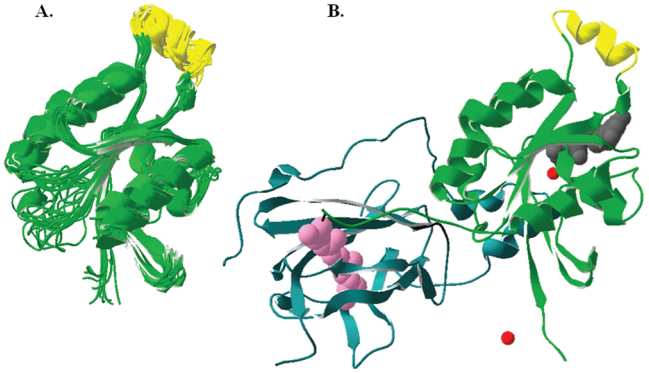

[a]Cdc42 is shown as a green ribbon with the Rho-insert domain colored yellow. (A) Superposition of the 12 most stable conformations of Cdc42 in solution, in the absence of nucleotide, determined by NMR (PDB entry 2KB0).[36] (B) Crystal structure of the RhoGDI−Cdc42 complex.[9]Cdc42 is colored green; GDP is colored gray, and Mg^{2+} ions are colored red. RhoGDI is colored turquoise and the GER moiety pink. Note how far the GER binding site is from the Rho-insert domain of Cdc42.

In our research, we simulated the structure of the RhoGDI−Cdc42 complex in solution (starting from a crystal structure), with emphasis on the correlation between the conformation of the Rho-insert helix of Cdc42 and the interactions of the lipid moiety with the immunoglobulin-like domain of RhoGDI.[9,43] As we will demonstrate, the RI helix is capable of acquiring greater freedom of motion, together with a loss of rigidity, with respect to the main body of the protein. This reordering of the domain was found to be a function of the interaction of the GER moiety with the RhoGDI protein that forms the complex with the Rho protein. Whenever the isoprene moiety is properly inserted into the RhoGDI's cleft, the Rho-insert deviates from the canonical conformation. To ascertain that the loss of the canonical structure of the Rho-insert is a function of an allosteric interaction of the hydrophobic moiety with RhoGDI, we introduced in silico mutations into the RhoGDI protein, replacing two key residues in its GER binding sites (L77A and I177N);[9,43] the latter mutation was demonstrated to lower (in vitro) the affinity of RhoGDI for the Rho protein and to enhance the tendency (in vivo) to develop metastasis.[44] In parallel, we also simulated a vacant RhoGDI−Cdc42 complex, in which the GER moiety was removed and the space spontaneously filled with solvent molecules. These simulations revealed that the solution structure of the RhoGDI−Cdc42 complex could readily retain the canonical orientation as in the crystalline form, but the insertion of the GER moiety destabilized the canonical orientation, leading to reorientation of the helix, loss of helical structure, or a combination of both. Apparently, the GER binding site of the RhoGDI proteins has additional function besides providing energy compensation for the removal of the GER from the membrane; through an allosteric interaction, it modulates the conformation of the signaling Rho-insert domain, informing the downstream proteins that Rho is in its inactive form.

METHODS

The molecular dynamics (MD) simulations were performed using the GROMACS 4 package of programs[45−49] using a force field of the GROMOS96 ffG53A6 force field.[50] The initial structure used for the simulations was the crystal structure of the RhoGDI−Cdc42 complex[9] (crystallized in the presence of GDP and two Mg^{2+} ions), which was downloaded from the Protein Data Bank[51] (PDB entry 1DOA). This well-resolved structure (2.6 Å) includes the isoprenylated Cdc42 and the insertion of this moiety into the hydrophobic pocket at the C-terminal β-sandwich-like immunoglobulin domain of RhoGDI. The parameters for the Mg^{2+} ions were those of the GROMOS96 ffG53A6 force field.

The parameters of the GDP molecule (bond lengths, angles, dihedral angles, improper angles, and partial charges) were taken from the GROMACS standard building blocks for ADP and guanine. The net charge of GDP was −2e.[50]

The topology of the GER moiety as needed for the simulation was generated by the using the PRODRG server (http://davapc1.bioch.dundee.ac.uk/cgi-bin/prodrg_beta)[52,53] (see also refs 54 and 55). The bonds, angles, and dihedral angles were checked for compatibility with the ffG53a6 force field parameters. The net charge of the GER moiety was zero.

The proteins were embedded in a box containing the SPC water model[56] that extended to at least 12 Å between the protein and the edge of the box. Na^+ and Cl^- ions were added to neutralize the protein's charges and to bring the ionic strength to ∼100 mM. Prior to the simulations, internal constraints were relaxed by energy minimization. Following the minimization, a 50 ps equilibration run was conducted under position restraints of heavy atoms (1000 kJ mol^{-1} nm^{-2}). Following that step, an MD production run was performed. During the MD run, the LINCS algorithm[57] was used to constrain the lengths of all bonds; the water molecules were restrained using the SETTLE algorithm.[58] The time step for the simulations was 2 fs (0.002 ps). The simulations were conducted under constant-pressure and -temperature (NPT) conditions, using Berendsen's coupling algorithm to keep the temperature and pressure constant (P = 1 bar; τ_p = 0.5 ps; T =

Table 1. Components Present in the Molecular Dynamics Simulations of the RhoGDI−Cdc42 Complex

simulated structure	time (ns)	no. of ions	no. of water molecules	protein	average rmsd for Cα atoms of the protein (nm)	canonical conformation of Rho-insert
holo 1 complex (C1.1)	50	39 Na^+, 34 Cl^-	18798	RhoGDI	0.31 ± 0.03	
				Cdc42	0.31 ± 0.04	no
holo 2 complex (C1.2)	50	39 Na^+, 34 Cl^-	18798	RhoGDI	0.34 ± 0.05	
				Cdc42	0.30 ± 0.07	no
holo 3 complex (C1.3)	50	39 Na^+, 34 Cl^-	18798	RhoGDI	0.37 ± 0.04	
				Cdc42	0.26 ± 0.03	no
apo complex, no GER (C2)	40	40 Na^+, 34 Cl^-	18815	RhoGDI	0.37 ± 0.03	
				Cdc42	0.22 ± 0.01	yes
Cdc42−$RhoGDI_{L77A}$ complex (C3)	50	39 Na^+, 34 Cl^-	18792	RhoGDI	0.33 ± 0.04	
				Cdc42	0.26 ± 0.03	yes
Cdc42−$RhoGDI_{I177N}$ complex (C4)	40	39 Na^+, 34 Cl^-	18796	RhoGDI	0.36 ± 0.07	
				Cdc42	0.24 ± 0.02	yes

300 K; τ_T = 0.1 ps).[59] The VdW forces were treated using a 10 Å cutoff. Long-range electrostatics were treated using the PME (particle mesh Ewald) method.[60] The coordinates were saved every 2 ps.

Cluster Analysis. Cluster analysis was performed using the GROMOS algorithm with a root-mean-square deviation (rmsd) cutoff value of 0.18 nm.[61]

Visualization. The figures were generated with VMD[62] and Swiss-PdbViewer.[63]

RESULTS AND DISCUSSION

Molecular Dynamics Simulations of the RhoGDI−Cdc42 Complex. The simulations conducted in this study were of the RhoGDI−Cdc42 complex, and structural analysis was conducted for each of the proteins. Six simulations were conducted using six initial states that all derived from the same crystal structure (see Table 1 for details). Simulations (C1.1, C1.2, and C1.3) were repetitive runs of the native structure of the complex without any modifications. These simulations differed by only the initial random distribution of the velocities. For simulation C2, the GER moiety was eliminated from the binding site and the space was spontaneously filled by water molecules that had penetrated the cavity during the initial relaxation of the structure prior to initiation of the simulation. Simulations C3 and C4 were of the holo complex, with the RhoGDI protein subjected to in silico mutations L77A and I177N, respectively. The mutations were limited to the hydrophobic binding sites of RhoGDI, adjacent to the β-sandwich-like immunoglobulin domain and cupped by the C-terminal region. Two mutants were selected; in one, the leucine moiety L77 was replaced with alanine (L77A). This mutation was selected because an equivalent mutation in a homologous protein, galectin-1 (L11A), reduced its affinity for the H-Ras protein.[64] The L77 residue in RhoGDI is located at the bottom of the hydrophobic cavity, close to the free end of the GER moiety, and displays the largest surface area in contact with the GER moiety. Moreover, L77 was shown to be a key player in the dramatic structural change of the hydrophobic pocket of RhoGDI, the formation of the Cdc42−RhoGDI complex.[9] The second mutation, I177N, was selected because it lowered the binding affinity for the Cdc42 protein[43] and enhanced the tendency of mutated animals to develop metastasis.[44] The replacement of the hydrophobic group of isoleucine with the more polar asparagine reduced the binding affinity for Rho proteins by up to 20-fold.[65] These two mutations are expected to weaken the affinity of the GER molecule for the site.[44,64,65] MD simulations of the RhoGDI protein with a GER moiety indicated that the GER can exercise some rocking motions at its binding site. Both of the mutations largely enhanced the amplitude of this motion (A. Abramovitz, Ph.D. Thesis, 2011).

The rmsd values, calculated for the Cα atoms for each protein in the RhoGDI−Cdc42 complex, are listed in Table 1, indicating that both proteins (RhoGDI and Cdc42) exhibited comparable structural fluctuations and the variations between the runs were within the standard deviations.

Quantitative Expression of the Structural Fluctuation of Cdc42 in the Holo RhoGDI−Cdc42 Complex. Figure 1 depicts the root-mean-square fluctuation (rmsf) of the Cα atoms of Cdc42 during the simulations listed in Table 1.

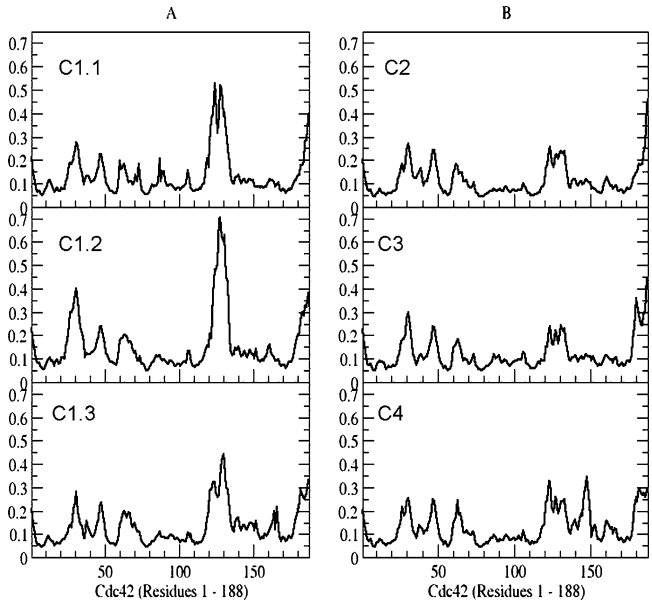

Figure 1. rmsf plot calculated for the Cα atoms of the Cdc42 protein as calculated for the simulations listed in Table 1. The *y* axis denotes the rmsd values in nanometers. The *x* axis denotes the sequence of the amino acids of the protein. The names of the simulations are included.

Basically, the rmsf function of Cdc42 is rather low, where the well-structured elements, helices and strands, have values of ≪1 Å. The loops connecting the structural elements and the N- and C-termini are naturally freer to fluctuate. What was surprising was the observation that the Rho-insert helix (residues 121−134 of Cdc42) appeared to have a very high value, especially in

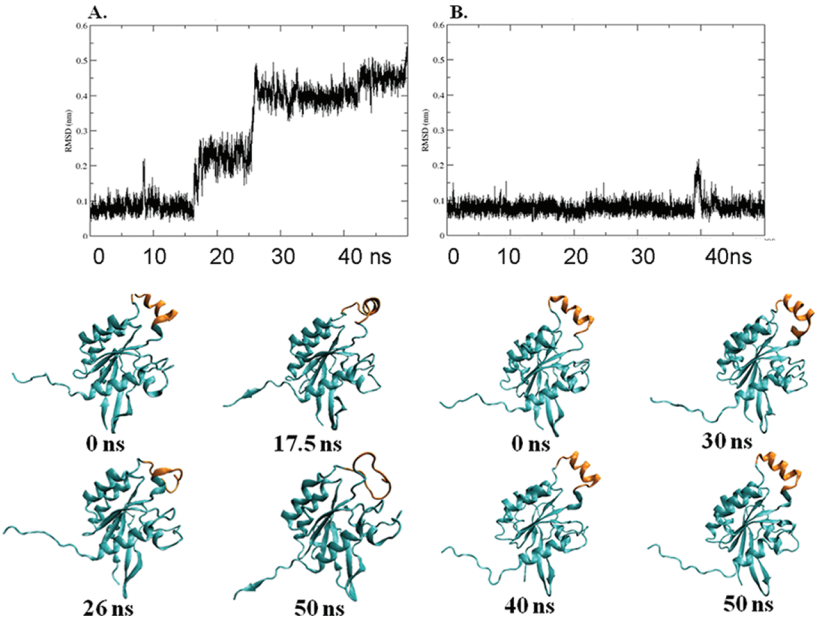

Figure 2. (A) rmsd of the Cα atoms of the Rho-insert domain of the Cdc42 protein in simulation C1.2. Below are four snapshots of the protein depicting the rotation and/or deformation of the Rho-insert domain at the indicated time points. For the sake of clarity, the Rho-insert region is colored orange. (B) rmsd of the Cα atoms of the Rho-insert domain of the Cdc42 protein in simulation C3. Below are four snapshots of the protein depicting the Rho-insert domain.

the holo complexes, where the GER moieties are expected to have an unperturbed interaction with the RhoGDI protein. These fluctuations in the Rho-insert exceeded the standard error of the fluctuations (Figure S1 of the Supporting Information). Upon calculation of the rmsf parameters for the last 10 ns of the simulation time, well after the structural fluctuation of the Rho-insert was complete, the rmsf of the Rho-insert domain was as stable as those of the other helices, indicating that the domain had reached a new stable configuration. Apparently, it seems that the presence of the GER in the GDI hydrophobic binding site specifically affects the conformation of the Rho-insert helix of the Rho protein in its complex with RhoGDI.

Figure 2 depicts the rmsd function calculated only for the IR section in the Cdc42 protein calculation, as evaluated in simulation C1.2 of the holo complex and for the simulation of the mutant $RhoGDI_{L77A}$–Cdc42 complex (simulation C3). During the simulation of the holo complex (panel A), there are two events during which the value increased rapidly. The snapshots taken at these time points reveal a major structural deformation of the Rho-insert helix; at ∼17.5 ns, it exhibits an ∼90° rotation with respect to the rest of the protein, and at ∼26 ns, where another jump in the rmsd value took place, the Rho-insert practically lost its helix nature, gaining a random coil structure (Figure 2B). In contrast with these deformations, the trajectory at which the GER–RhoGDI interaction was impaired by insertion of an in silico L77A mutation, the rmsd of the Rho-insert was constant over the 50 ns of the simulation, and no distortion of the helix was observed. The other two simulations of the holo complex indicated that the rotation of the Rho-insert and the loss of the helix structure are independent events. In simulation C1.1, the helix was rotated but retained a helical structure, whereas in simulation C1.3, the helix gained a random coil structure without the rotation phase (Figures S2 and S3 of the Supporting Information). In simulations C2–C4, where the GER moiety was absent or its binding site was mutated, no changes in the Rho-insert helix were noticed over the whole length of the trajectory (Figures S4–S6 of the Supporting Information).

For comparison between the structural stability of the whole protein and that of the Rho-insert domain, we related in Figure 3 the rmsd of the Rho-insert domain (ordinate) to the rmsd of the rest of the protein (residues 1–120 and 135–188) as denoted on the abscissa. In such a presentation, the upward stretch of the data points indicates a higher mobility of the Rho-insert residues with respect to the rest of the protein. Of all simulations, the most stable Rho-insert structures were those of the two mutants (red and blue) that are almost overlapping

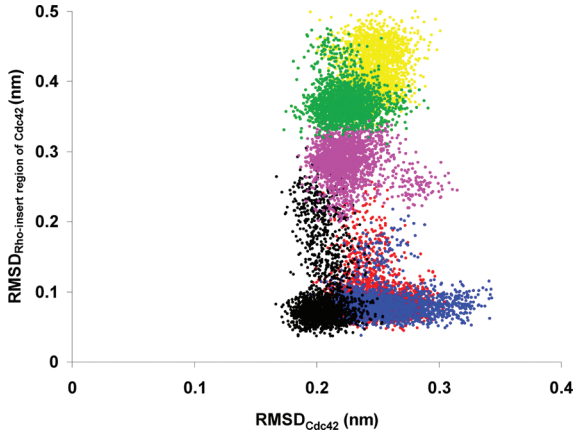

Figure 3. Comparison of the rmsd of the Cα atoms of the Rho-insert domain with the value calculated for the rest of the protein. The rmsd values were calculated for snapshots taken at 10 ps intervals for the last 20 ns of the simulations. The ordinate denotes the rmsd value of the Rho-insert domain (residues 121–134) and the abscissa the rmsd value of residues 1–120 and 135–188 of Cdc42. The color code for the simulations is as follows: green for C1.1, yellow for C1.2, purple for C1.3, black for C2, blue for C3, and red for C4.

dx.doi.org/10.1021/bi201211v | *Biochemistry* 2012, 51, 715–723

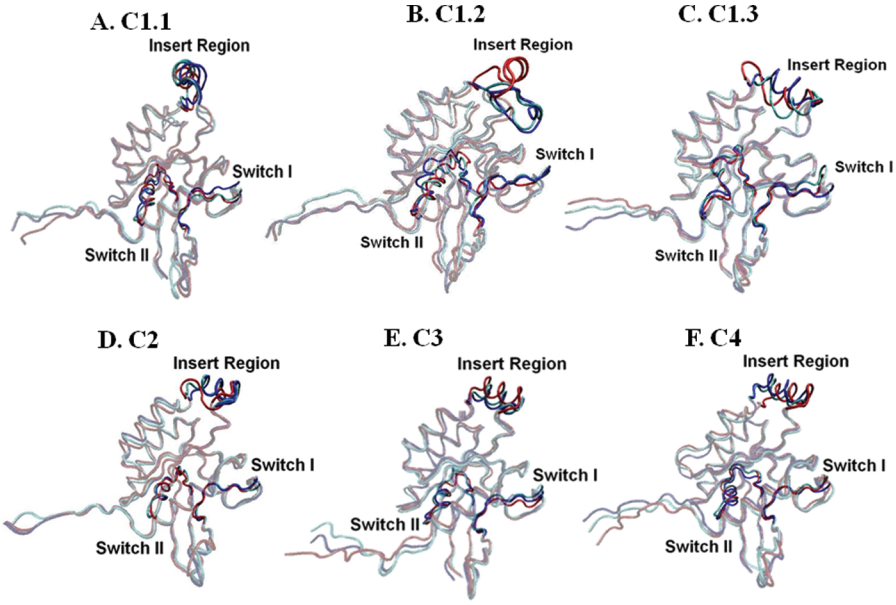

Figure 4. Superposition of the three largest clusters of Cdc42, depicted in turquoise, blue, and red. The clusters were defined by setting the cutoff value of the cluster analysis to Δrmsd = 0.18 nm.

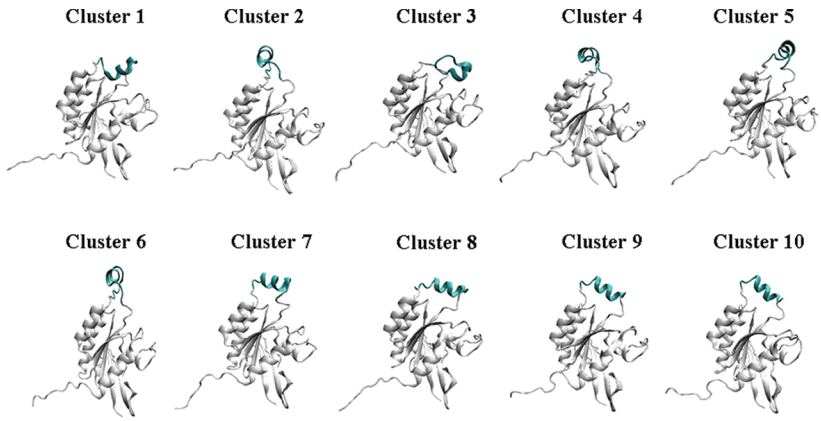

Figure 5. Structures of the 10 largest clusters of the Cdc42 protein. The structures were driven by cluster analysis of all the structures accumulated during 134 ns of simulation time of the three Cdc42–RhoGDI complexes. The relative contribution of each cluster to the total number of structures is given in Table 2. The Rho-insert domain is colored turquoise.

each other; the divergence of the data points for these simulations along the *y* axis is even smaller than on the *x* axis, meaning that the Rho-insert is even more stable than the rest of the protein. The Rho-insert domain of the apo complex, where the GER moiety was eliminated from the binding site (black), still retains a high stability. Most of the data points have *y* values smaller than those on the *x* axis. However, the three holo complexes (green, purple, and yellow) clearly differ with respect to all others; while the rmsd of the protein is still within the same range, the value of the Rho-insert increases significantly, indicating that the Rho-insert domain in these complexes had gained motional freedom.

In simulation C1.1, the rotation of the RI took place within the first 8 ns and the spread of the green data points corresponds to a "mature" reorientation of the RI domain. The yellow dots of simulation C1.2 are spread in the same direction as the first, indicating that a structural change in the RI region of Cdc42 has also occurred. Finally, in the trajectory of C.1.3, the structural transition occurs gradually, and the purple points are stretched over time, rising toward the level of the mature state.

Cluster Analysis of the Cdc42–RhoGDI Complex. The multitude of structures assumed by the proteins during the simulations was subjected to cluster analysis. By this procedure, all structures are sorted (by cross-rmsd values) into clusters; in each, all items are within a preset range (Δrmsd) from a representative structure. The value of Δrmsd was optimized to 0.18 nm, and the analysis was applied for the last 30 ns of all simulations. The results are given in Table S1 of the Supporting Information.

Figure 4 is a superposition of the three largest clusters of each of the simulations. In this presentation, the main body of the protein is presented in the same orientation, thus emphasizing the domains in which the largest structural fluctuation took place: the unstructured N- and C-termini, switch I, switch II, and, in some cases, the Rho-insert (see Figure 4).

In the top row of Figure 4, the Rho-insert domain, located atop each structure, had lost its canonical orientation, revealing

dx.doi.org/10.1021/bi201211v | *Biochemistry* 2012, 51, 715–723

either 90° rotation (A), rotation and the loss of helix structure (B), or partial gain of a random coil structure (C). In the other simulations, where the interaction between the GER and the RhoGDI protein was impaired, the canonical orientation was persistent in all clusters.

A recent study by Raimondi and co-workers was a comparative analysis of various guanine nucleotide binding proteins (ARF1, SEC4, H-Ras, RhoA, and $G\alpha_T$)[37] in their active (GTP-bound) state and inactive (GDP-bound) state. The simulations revealed a very high degree of similarity between the two states, as observed by the comparison of the first 20 eigenvectors derived by the principle component analysis of these structures. None of these structures deviated from the canonical orientation of the Rho-insert region. Thus, it seems that the noncanonical orientation, detected in our simulations, is specific for the solution structure of the native RhoGDI−Cdc42 complex.

Cluster Analysis of Holoprotein Simulations. The peculiar reorientation of the Rho-insert, noted for the holo complex simulations (C1.1−C1.3), was further investigated. Considering that the three simulations are repetitions of the same initial state, differing only in their initial velocities, we combined the trajectories (to eliminate the most initial relaxation from the crystal structure, the first 2 ns of the trajectory was not included in the analysis) and subjected the product to cluster analysis, summing 134 ns of total simulation time. The analysis (using snapshots taken at 20 ps intervals and a Δrmsd of 0.18 nm) generated 79 clusters, the largest of them containing ∼10% of the total population, a fair representation of the manifold states that the protein can assume. The structures, representing the first 10 clusters, are shown in Figure 5, and their characteristic properties are listed in Table 2.

Table 2. Size and Dynamic Properties of the 10 Largest Clusters of the Cdc42 Protein Calculated from the Combined Trajectories of Holo Complexes

average time (ps)	no. of transitions	% of total	no. of structures	cluster
172	80	10.6	691	1
112	118	9.9	664	2
599	18	8.0	539	3
107	70	5.6	376	4
308	24	5.5	370	5
50	140	5.2	353	6
77	78	4.4	301	7
81	64	3.9	262	8
201	24	3.6	242	9
139	34	3.5	237	10

During the simulation, the protein switched from one configuration to another at an average frequency of ∼5 ns^{-1}, and the average time that the protein conformed with a structure of a given cluster varied by ∼10-fold (i.e., cluster 3 vs cluster 6). The various clusters differed in their popularity and the average time that the structure was still within the characteristics of the host cluster. Thus, cluster 3 represents a configuration with an average lifetime of ∼600 ps, while the structures of cluster 6 lasted, on average, only ∼50 ps. The fast transition between the clusters implies that the system is in equilibrium, where the difference in the probability of adjacent configuration is compatible with $\Delta G \leq 1\ k_B T$ (∼0.6 kcal/mol). Apparently, none of the cluster functioned as a local trap on the free energy landscape.

Once we have established the ability of the proteins to sample the whole conformational space, there is a physical meaning for the shape of the representative structures of the clusters. Figure 5 depicts the representative structure of the first 10 clusters (comprising ∼60% of the total population), all equally oriented with respect to the main body of the protein. In contrast with the uniformity of the main body of the protein, the Rho-insert, colored turquoise, exhibits a large variability in shape and orientation, where the canonical shape[7,31,34,66] is limited to the smaller clusters, 7−10.

The persistent deviation of the Rho-insert, in the holo complex simulations, from its canonical configuration may be considered as an artifact. However, the inspection of the crystal structures of some plant Rho proteins ROP4, ROP5, and ROP7 reveals a similar noncanonical orientation (Figure 6).[27,39−42]

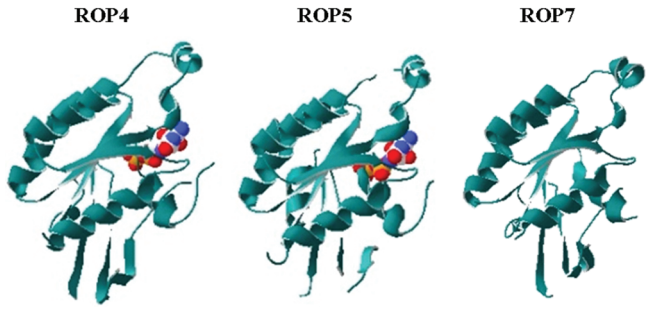

Figure 6. Crystal structure of the plant Rho proteins ROP4,[40] ROP5,[39] and ROP7[41] (PDB entries 2NTY, 3WBD, and 2WBL, respectively), which feature the noncanonical orientation of the Rho-insert in their crystal structure. The GDP molecule is represented by VdW radii and CPK coloring.

On the other hand, the ROP9 protein[27,67] retains the canonical orientation indicating that both are legitimate crystalline structures. It should be stressed that in all simulations where the interaction of the GER with the RhoGDI was impaired, none of the clusters (even the smallest ones) deviated from the canonical orientation. Apparently, the loss of the canonical orientation is not coincidental and is derived by a specific interprotein interaction.

Structural Fluctuation of the RhoGDI Protein in the Complex. The extensive study of Raimondi and co-workers,[37] comparing the structures of many small GTPase proteins, clearly indicated that in all cases the Rho-insert maintains its canonical conformation, implying that the effect noticed in our study is mediated by the RhoGDI in the complex. For this reason we compared the conformations of RhoGDI in the various runs.

Figure 7 depicts the first three largest clusters of RhoGDI in the simulations. Generally, the structures are much alike, only that in simulations C1.1−C1.3 the short helix at the N-terminus (present in the crystal structure of the complex) appeared to be rather stable while in all other runs, the structure was lost within the first nanosecond of the simulation time (see the marking in the figure). The persistence of this local ordered structure is a consequence of the tight interaction of GER with RhoGDI, allowing the N-terminal domain of RhoGDI to nicely cap the GER binding site. The mutations in the GER binding site or its omission destabilizes the domain, and the helix cannot be formed. It should be stated that in simulations of RhoGDI in its solution structure, the N-terminal helix was

dx.doi.org/10.1021/bi201211v | Biochemistry 2012, 51, 715−723

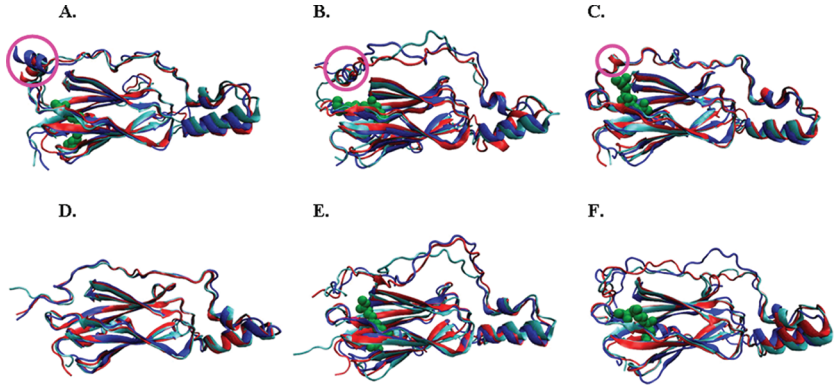

Figure 7. Superpositioned structures of the three largest clusters of the RhoGDI protein derived from cluster analysis of the simulations of the Cdc42−RhoGDI complexes. Panels A−F correspond to simulations C1.1, C1.2, C1.3, C2, C3, and C4, respectively. The GER moiety is colored green. The short helical section of residues 10−15 in the N-terminal domain of RhoGDI, present only in the holoprotein complex simulations, is marked by a circle.

unraveled within a few nanoseconds, as in panels D−F (Figure S5 of the Supporting Information).

CONCLUDING REMARKS

In this study, we investigated by MD simulations the solution structure of Cdc42, a member of the family of Rho guanine nucleotide binding proteins, in its complex with RhoGDI. This complex is the dominant form of the soluble inactive state of the protein.

The Rho-insert domain in the crystal structure of the Rho protein as well as the solution structure adheres to its canonical conformation, suggesting that this form is more stable than that appearing during the simulation of the RhoGDI−Cdc42 complex. The analysis of these simulations reveals a fascinating coupling between the orientation integrity of the Rho-insert domain of Cdc42 and the proper insertion of the GER moiety of Cdc42 into the hydrophobic binding site of RhoGDI, some 60 Å away.[8,9] Apparently, there is an allosteric yet specific coupling between reactive sites on a protein that can propagate over a long distance.

The Rho-insert domain had been identified as a signaling element, as it has almost no effect on the rate of GTP hydrolysis[29−31] but appears to be essential for downstream signaling.[32,34] The fact that the Rho-insert helix retains identical orientation in the GTP (active) and GDP (inactive) states of the protein[37] implies that the reorientation is not coupled with the activity of the protein, but most probably with the signaling function, indicating to downstream protein that the Rho is in an inactive state. Simulations of another member of the Rho proteins, Rac1 in its complex with RhoGDI 1 (PDB entry 1HH4), reveal a similar behavior: when the GER moiety of Rac1 was inserted into the hydrophobic cavity of RhoGDI1, the Rho-insert was rotated and lost most of its helical structure, yet in the case where the GER was omitted and the cavity was filled with water, the canonical orientation was strictly conserved (see Figure S6 of the Supporting Information). This observation confirms the generality of the phenomenon.

ASSOCIATED CONTENT

Supporting Information

Six figures and one table. This material is available free of charge via the Internet at http://pubs.acs.org.

AUTHOR INFORMATION

Corresponding Author

*E-mail: eti@hplus.tau.ac.il. Telephone: +97236409824.

ABBREVIATIONS

RI, Rho-insert domain of Rho proteins; GER, geranylgeranyl; GDP, guanosine diphosphate; MD, molecular dynamics; VdW, van der Waals; LINCS, Linear Constraint Solver algorithm; SPC, simple point charge; PDB, Protein Data Bank.

REFERENCES

(1) Johnson, D. I. (1999) Cdc42: An essential Rho-type GTPase controlling eukaryotic cell polarity. *Microbiol. Mol. Biol. Rev. 63* (1), 54−105.

(2) Ridley, A. J. (2006) Rho GTPases and actin dynamics in membrane protrusions and vesicle trafficking. *Trends Cell Biol. 16* (10), 522−529.

(3) Etienne-Manneville, S., and Hall, A. (2002) Rho GTPases in cell biology. *Nature 420* (6916), 629−635.

(4) Wennerberg, K., Rossman, K. L., and Der, C. J. (2005) The Ras superfamily at a glance. *J. Cell Sci. 118* (Part 5), 843−846.

(5) Lane, K. T., and Beese, L. S. (2006) Thematic review series: Lipid posttranslational modifications. Structural biology of protein farnesyltransferase and geranylgeranyltransferase type I. *J. Lipid Res. 47* (4), 681−699.

(6) Pechlivanis, M., and Kuhlmann, J. (2006) Hydrophobic modifications of Ras proteins by isoprenoid groups and fatty acids: More than just membrane anchoring. *Biochim. Biophys. Acta 1764* (12), 1914−1931.

(7) Gosser, Y. Q., Nomanbhoy, T. K., Aghazadeh, B., Manor, D., Combs, C., Cerione, R. A., and Rosen, M. K. (1997) C-terminal binding domain of Rho GDP-dissociation inhibitor directs N-terminal inhibitory peptide to GTPases. *Nature 387* (6635), 814−819.

(8) Keep, N. H., Barnes, M., Barsukov, I., Badii, R., Lian, L. Y., Segal, A. W., Moody, P. C., and Roberts, G. C. (1997) A modulator of rho family G proteins, rhoGDI, binds these G proteins via an immunoglobulin-like domain and a flexible N-terminal arm. *Structure 5* (5), 623−633.

(9) Hoffman, G. R., Nassar, N., and Cerione, R. A. (2000) Structure of the Rho family GTP-binding protein Cdc42 in complex with the multifunctional regulator RhoGDI. *Cell 100* (3), 345−356.

(10) Grizot, S., Faure, J., Fieschi, F., Vignais, P. V., Dagher, M. C., and Pebay-Peyroula, E. (2001) Crystal structure of the Rac1-RhoGDI complex involved in NADPH oxidase activation. *Biochemistry 40* (34), 10007−10013.

(11) Longenecker, K., Read, P., Derewenda, U., Dauter, Z., Liu, X., Garrard, S., Walker, L., Somlyo, A. V., Nakamoto, R. K., Somlyo, A. P.,

et al. (1999) How RhoGDI binds Rho. *Acta Crystallogr. D55* (Part 9), 1503−1515.
(12) Scheffzek, K., Stephan, I., Jensen, O. N., Illenberger, D., and Gierschik, P. (2000) The Rac-RhoGDI complex and the structural basis for the regulation of Rho proteins by RhoGDI. *Nat. Struct. Biol. 7* (2), 122−126.
(13) Boulter, E., and Garcia-Mata, R. (2010) RhoGDI: A rheostat for the Rho switch. *Small Gtpases 1* (1), 65−68.
(14) Boulter, E., Garcia-Mata, R., Guilluy, C., Dubash, A., Rossi, G., Brennwald, P. J., and Burridge, K. (2010) Regulation of Rho GTPase crosstalk, degradation and activity by RhoGDI1. *Nat. Cell Biol. 12* (5), 477−483.
(15) Dovas, A., and Couchman, J. R. (2005) RhoGDI: Multiple functions in the regulation of Rho family GTPase activities. *Biochem. J. 390* (Part 1), 1−9.
(16) Olofsson, B. (1999) Rho guanine dissociation inhibitors: Pivotal molecules in cellular signalling. *Cell. Signalling 11* (8), 545−554.
(17) DerMardirossian, C., and Bokoch, G. M. (2005) GDIs: Central regulatory molecules in Rho GTPase activation. *Trends Cell Biol. 15* (7), 356−363.
(18) Loh, A. P., Guo, W., Nicholson, L. K., and Oswald, R. E. (1999) Backbone dynamics of inactive, active, and effector-bound Cdc42Hs from measurements of ^{15}N relaxation parameters at multiple field strengths. *Biochemistry 38* (39), 12547−12557.
(19) Bouguet-Bonnet, S., and Buck, M. (2008) Compensatory and long-range changes in picosecond-nanosecond main-chain dynamics upon complex formation: ^{15}N relaxation analysis of the free and bound states of the ubiquitin-like domain of human plexin-B1 and the small GTPase Rac1. *J. Mol. Biol. 377* (5), 1474−1487.
(20) Bishop, A. L., and Hall, A. (2000) Rho GTPases and their effector proteins. *Biochem. J. 348* (Part 2), 241−255.
(21) Wennerberg, K., and Der, C. J. (2004) Rho-family GTPases: It's not only Rac and Rho (and I like it). *J. Cell Sci. 117* (Part 8), 1301−1312.
(22) Adams, P. D., and Oswald, R. E. (2006) Solution structure of an oncogenic mutant of Cdc42Hs. *Biochemistry 45* (8), 2577−2583.
(23) Adams, P. D., and Oswald, R. E. (2007) NMR assignment of Cdc42(T35A), an active Switch I mutant of Cdc42. *Biomol. NMR Assignments 1* (2), 225−227.
(24) Lammers, M., Meyer, S., Kuhlmann, D., and Wittinghofer, A. (2008) Specificity of interactions between mDia isoforms and Rho proteins. *J. Biol. Chem. 283* (50), 35236−35246.
(25) Somesh, B. P., Neffgen, C., Iijima, M., Devreotes, P., and Rivero, F. (2006) *Dictyostelium* RacH regulates endocytic vesicular trafficking and is required for localization of vacuolin. *Traffic 7* (9), 1194−1212.
(26) Thapar, R., Karnoub, A. E., and Campbell, S. L. (2002) Structural and biophysical insights into the role of the insert region in Rac1 function. *Biochemistry 41* (12), 3875−3883.
(27) Thomas, C., and Berken, A. (2010) Structure and Function of ROPs and their GEFs. *Integrated G Proteins Signaling in Plants,*, 49−69.
(28) Tu, S., and Cerione, R. A. (2001) Cdc42 is a substrate for caspases and influences Fas-induced apoptosis. *J. Biol. Chem. 276* (22), 19656−19663.
(29) Walker, S. J., and Brown, H. A. (2002) Specificity of Rho insert-mediated activation of phospholipase D1. *J. Biol. Chem. 277* (29), 26260−26267.
(30) Walker, S. J., Wu, W. J., Cerione, R. A., and Brown, H. A. (2000) Activation of phospholipase D1 by Cdc42 requires the Rho insert region. *J. Biol. Chem. 275* (21), 15665−15668.
(31) Wu, W.-J., Leonard, D. A., Cerione, R. A., and Manor, D. (1997) Interaction between Cdc42Hs and RhoGDI is mediated through the Rho insert region. *J. Biol. Chem. 272* (42), 26153−26158.
(32) Wu, W. J., Tu, S., and Cerione, R. A. (2003) Activated Cdc42 sequesters c-Cbl and prevents EGF receptor degradation. *Cell 114* (6), 715−725.
(33) Dorjgotov, D., Jurca, M. E., Fodor-Dunai, C., Szucs, A., Otvos, K., Klement, E., Biro, J., and Feher, A. (2009) Plant Rho-type (Rop) GTPase-dependent activation of receptor-like cytoplasmic kinases in vitro. *FEBS Lett. 583* (7), 1175−1182.
(34) Wu, W. J., Lin, R., Cerione, R. A., and Manor, D. (1998) Transformation activity of Cdc42 requires a region unique to Rho-related proteins. *J. Biol. Chem. 273* (27), 16655−16658.
(35) Feltham, J. L., Dotsch, V., Raza, S., Manor, D., Cerione, R. A., Sutcliffe, M. J., Wagner, G., and Oswald, R. E. (1997) Definition of the switch surface in the solution structure of Cdc42Hs. *Biochemistry 36* (29), 8755−8766.
(36) Chandrashekar, R., Salem, O., Krizova, H., McFeeters, R., and Adams, P. D. (2011) A switch I mutant of cdc42 exhibits less conformational freedom. *Biochemistry 50* (28), 6196−6207.
(37) Raimondi, F., Portella, G., Orozco, M., and Fanelli, F. (2011) Nucleotide binding switches the information flow in ras GTPases. *PLoS Comput. Biol. 7* (3), e1001098.
(38) Dvorsky, R., and Ahmadian, M. R. (2004) Always look on the bright site of Rho: Structural implications for a conserved intermolecular interface. *EMBO Rep. 5* (12), 1130−1136.
(39) Thomas, C., and Berken, A. (2007) Purification, crystallization and preliminary X-ray diffraction analysis of the plant Rho protein ROP5. *Acta Crystallogr. F63* (Part 12), 1070−1072.
(40) Thomas, C., Fricke, I., Scrima, A., Berken, A., and Wittinghofer, A. (2007) Structural evidence for a common intermediate in small G protein-GEF reactions. *Mol. Cell 25* (1), 141−149.
(41) Thomas, C., Fricke, I., Weyand, M., and Berken, A. (2009) 3D structure of a binary ROP-PRONE complex: The final intermediate for a complete set of molecular snapshots of the RopGEF reaction. *Biol. Chem. 390* (5−6), 427−435.
(42) Thomas, C., Weyand, M., Wittinghofer, A., and Berken, A. (2006) Purification and crystallization of the catalytic PRONE domain of RopGEF8 and its complex with Rop4 from *Arabidopsis thaliana*. *Acta Crystallogr. F62* (Part 6), 607−610.
(43) Hoffman, G. R., and Cerione, R. A. (2004) Regulation of the RhoGTPases by RhoGDI. *Rho GTPases,*, 32−45.
(44) Moissoglu, K., McRoberts, K. S., Meier, J. A., Theodorescu, D., and Schwartz, M. A. (2009) Rho GDP dissociation inhibitor 2 suppresses metastasis via unconventional regulation of RhoGTPases. *Cancer Res. 69* (7), 2838−2844.
(45) Van der Spoel, D., Lindahl, E., Hess, B., Groenhof, G., Mark, A. E., and Berendsen, H. J. C. (2005) GROMACS: Fast, flexible, and free. *J. Comput. Chem. 26* (16), 1701−1718.
(46) van Der Spoel, D., Lindahl, E., Hess, B., van Buuren, A. R., Apol, E., Meulenhoff, P. J., Tieleman, D. P., Sijbers, A. L. T. M., Feenstra, A. K., van Drunen, R., et al. (2004) *GROningen Machine for Molecular Simulations*, version 3.2.1, University of Groningen, Groningen, The Netherlands.
(47) Berendsen, H. J. C., van der Spoel, D., and van Drunen, R. (1995) GROMACS: A message-passing parallel molecular dynamics implementation. *Comput. Phys. Commun. 91*, 43−56.
(48) Hess, B., Kutzner, C., van der Spoel, D., and Lindahl, E. (2008) GROMACS 4: Algorithms for highly efficient, load-balanced, and scalable molecular simulation. *J. Chem. Theory Comput. 4* (3), 435−447.
(49) Lindahl, E., Hess, B., and van der Spoel, D. (2001) GROMACS 3.0: A package for molecular simulation and trajectory analysis. *J. Mol. Model. 7* (8), 306−317.
(50) Oostenbrink, C., Villa, A., Mark, A. E., and van Gunsteren, W. F. (2004) A biomolecular force field based on the free enthalpy of hydration and solvation: The GROMOS force-field parameter sets 53A5 and 53A6. *J. Comput. Chem. 25* (13), 1656−1676.
(51) Berman, H. M., Westbrook, J., Feng, Z., Gilliland, G., Bhat, T. N., Weissig, H., Shindyalov, I. N., and Bourne, P. E. (2000) The Protein Data Bank. *Nucleic Acids Res. 28* (1), 235−242.
(52) Schuttelkopf, A. W., and van Aalten, D. M. (2004) PRODRG: A tool for high-throughput crystallography of protein-ligand complexes. *Acta Crystallogr. D60* (Part 8), 1355−1363.
(53) van Aalten, D. M., Bywater, R., Findlay, J. B., Hendlich, M., Hooft, R. W., and Vriend, G. (1996) PRODRG, a program for generating molecular topologies and unique molecular descriptors from coordinates of small molecules. *J. Comput.-Aided Mol. Des. 10* (3), 255−262.

(54) Vandermoten, S., Santini, S., Haubruge, E., Heuze, F., Francis, F., Brasseur, R., Cusson, M., and Charloteaux, B. (2009) Structural features conferring dual geranyl/farnesyl diphosphate synthase activity to an aphid prenyltransferase. *Insect Biochem. Mol. Biol. 39* (10), 707−716.
(55) Siwko, M. E., Marrink, S. J., de Vries, A. H., Kozubek, A., Schoot Uiterkamp, A. J., and Mark, A. E. (2007) Does isoprene protect plant membranes from thermal shock? A molecular dynamics study. *Biochim. Biophys. Acta 1768* (2), 198−206.
(56) Berendsen, H. J. C., Postma, J. P. M., van Gunsteren, W. F., and Hermans, J. (1969) Interaction Models for Water in Relation to Protein Hydration. *Nature 224*, 175−177.
(57) Hess, B., Bekker, H., Berendsen, H. J. C., and Fraaije, J. G. E. M. (1997) LINCS: A linear constraint solver for molecular simulations. *J. Comput. Chem. 18*, 1463−1472.
(58) Miyamoto, S., and Kollman, P. A. (1992) SETTLE: An Analytical Version of the SHAKE and RATTLE Algorithms for Rigid water models. *J. Comput. Chem. 13*, 952−962.
(59) Berendsen, H. J. C., Postma, J. P. M., DiNola, A., and Haak, J. R. (1984) Molecular dynamics with coupling to an external bath. *J. Chem. Phys. 81*, 3684−3690.
(60) Essmann, U., Perera, L., Berkowitz, M. L., Darden, T., Lee, H., and Pedersen, L. G. (1995) A smooth particle mesh Ewald method. *J. Chem. Phys. 103* (19), 8577−8593.
(61) Daura, X., van Gunsteren, W. F., and Mark, A. E. (1999) Folding-unfolding thermodynamics of a β-heptapeptide from equilibrium simulations. *Proteins 34* (3), 269−280.
(62) Humphrey, W., Dalke, A., and Schulten, K. (1996) VMD: Visual molecular dynamics. *J. Mol. Graphics 14* (1), 27−38.
(63) Guex, N., and Peitsch, M. C. (1997) SWISS-MODEL and the Swiss-PdbViewer: An environment for comparative protein modeling. *Electrophoresis 18* (15), 2714−2723.
(64) Rotblat, B., Niv, H., Andre, S., Kaltner, H., Gabius, H. J., and Kloog, Y. (2004) Galectin-1(L11A) predicted from a computed galectin-1 farnesyl-binding pocket selectively inhibits Ras-GTP. *Cancer Res. 64* (9), 3112−3118.
(65) Platko, J. V., Leonard, D. A., Adra, C. N., Shaw, R. J., Cerione, R. A., and Lim, B. (1995) A single residue can modify target-binding affinity and activity of the functional domain of the Rho-subfamily GDP dissociation inhibitors. *Proc. Natl. Acad. Sci. U.S.A. 92* (7), 2974−2978.
(66) Lin, Q., Fuji, R. N., Yang, W., and Cerione, R. A. (2003) RhoGDI is required for Cdc42-mediated cellular transformation. *Curr. Biol. 13* (17), 1469−1479.
(67) Sormo, C. G., Leiros, I., Brembu, T., Winge, P., Os, V., and Bones, A. M. (2006) The crystal structure of *Arabidopsis thaliana* RAC7/ROP9: The first RAS superfamily GTPase from the plant kingdom. *Phytochemistry 67* (21), 2332−2340.